AN INVESTIGATION INTO THE FLOW AT THE JUNCTION BETWEEN A FLAT PLATE AND AN AEROFOIL

D Abdulrazak

and

*D R Philpott

School of Engineering, Hatfield Polytechnic
Hatfield, UK

Abstract

Traverses behind the trailing edge of a NACA 0018 wing mounted on a flat plate at zero incidence have been made and contour plots of vorticity and total pressure are presented together with flow visualisation of the wake region.

Nomenclature

U	free stream speed
P	pressure
ρ	air density
δ	probe radius
k	dimensionless yawmeter calibration factor
u	local velocity in x-axis
v	local velocity in y-axis
w	local velocity in z-axis
ζ	vorticity along the x-axis
Vo	local velocity at centre of vorticity probe in y-axis
Wo	local velocity at centre of vorticity probe in z-axis
Δp	differential pressure
X	a distance, parallel to flow
Y	a distance, width of the model
Z	a distance, height of the model
ψ	yaw angle
α	incidence angle
Re	Reynolds number
C	cord

1. Introduction

The flow in the region of a wing/body junction is characterised by a vortex generated by the interaction of the boundary layers on the body and on the wing. This interaction is of practical importance because the vortex system so produced provides a noticeable contribution to the overall drag of the wing. A proper understanding of the flow mechanisms involved is thus likely to lead to worthwhile improvements in performance.

A number of studies of this phenomenon have been made (eg Refs 1 and 2). The aim of the present investigation is to develop experimental and theoretical methods of analysing the flow in order, in the long term, to investigate the effect of fillet geometries at the junction.

This paper describes the development of a flow traverse system to measure local properties in the flowfield downstream of such a junction, including local vorticity. Results are presented for the flow round a NACA 0018 section mounted on a flat plate in a low speed wind tunnel.

2. Nature of the Junction Flow and Test Configuration

The main feature of the flow in the region of the junction is the formation of a horseshoe vortex. Air which has traversed through the fuselage boundary layer achieves a lower stagnation pressure when brought to rest at the wing leading edge than air which reaches the leading edge stagnation point at a position outboard of the wing root. A positive pressure gradient is thus generated in the z direction (Fig 1) and this induces a flow towards the root of the wing which rolls up to form the horseshoe vortex referred to above.

In order to gain insight into the processes involved, it is advantageous to study simplified cases. Some previous studies (eg Refs 2, 3, 5 and 6) have therefore chosen to replace the fuselage with a flat plate aligned to the flow and the wing has been replaced by a second thick flat plate with a rounded leading edge designed to simulate the conditions at the leading edge of a typical wing.

One feature which is of interest is the apparent spreading of the wake region immediately downstream of the trailing edge (Fig 2) and the present work is directed specifically at the flow in this region. Because of this it was decided to employ an aerofoil section with a sharp trailing edge while still retaining the simplification of the flat plate representation of the boundary layer.

The configuration chosen is illustrated in Fig 3. It consists of a NACA 0018 section wing, constructed of wood, mounted on a 6mm dural plate 1m long and .6m wide. Surface pressure tappings were provided on the plate surface. A transition strip was attached near the rounded leading edge. The wing was mounted centrally with its leading edge 0.37m from the leading edge of the plate and had a chord of 0.246m and a span of 0.4m.

The model was tested in the Hatfield Polytechnic 1.5m x 1.2m closed working section, open return tunnel which has a maximum speed of 25 m/s.

* Reader, Aerospace Engineering
Member of AIAA

3. Flow visualisation tests

Before deciding on the region in which the detailed flow traverses were to be made it was decided to conduct flow visualisation tests in order to identify the areas of principle interest. Fig 4 shows the result of an oil flow investigation. A thin mixture of kerosine, oleic acid and poster paint was painted on to the surface of the plate immediately upstream of the intersection region and on the leading edge of the wing. Different colours were used on the wing and the plate.

The resultant pattern is shown in Fig 4. The vortex trace on the plate surface could be clearly identified together with the divergent wake region. The use of the two colours revealed that the oil on the plate surface within the interaction region originated from the wing.

In addition to the oil flow test, surface tufts were also employed (Fig 5) and the extent of the vortex flowing in y-z planes was determined using a tuft grid.

4. Vorticimeter and Traverse

4.1 Traverse Mechanism

The traverse mechanism was a three axis system driven by stepper motors on each axis. Motion was achieved via lead screws and the resolution obtainable was approximately 0.1mm. The mechanism was controlled by means of an IBM XT computer and this machine was also used to acquire the data at each measurement point via a Dash 16 A-D board. The probe location is shown in Fig 6 and an outline of the control system is shown in Fig 7.

Traverses were made at a total of 15 planes at distances from the trailing edge of the wing ranging from 0.035m to 0.335m. At each plane passes were made in the y direction for a number of discrete values of z.

4.2 The Vorticimeter

In order to measure local values of vorticity, an eight tube yawmeter array was used (Fig 8) following the pattern outlined by Freestone (Ref 7). Freestone relates the pressure difference produced by each yawmeter pair to the local velocity gradients as:

$$p_2 - p_3 = K.\frac{1}{2}.\rho.(U + \delta.\frac{\partial u}{\partial z}).(V_0 + \frac{\partial v}{\partial z})$$

$$p_5 - p_4 = K.\frac{1}{2}.\rho.(U + \delta.\frac{\partial u}{\partial y}).(W_0 + \frac{\partial w}{\partial y})$$

$$p_7 - p_6 = K.\frac{1}{2}.\rho.(U - \delta.\frac{\partial u}{\partial z}).(V_0 - \delta.\frac{\partial v}{\partial z})$$

$$p_8 - p_1 = K.\frac{1}{2}.\rho.(U + \delta.\frac{\partial u}{\partial y}).(W_0 - \delta.\frac{\partial w}{\partial y}) \quad \text{.....(1)}$$

This yields:

$$\sum_{i\ odd} p_i - \sum_{i\ even} p_i = \frac{1}{2}.\rho.K.2.\delta.U.(\frac{\partial w}{\partial y} - \frac{\partial v}{\partial z}) \quad \text{.....(2)}$$

If the values of u/y and u/z are small, then equation 2 becomes:

$$\Delta\sum p = K.\rho.\delta.U.\zeta_x \quad \text{.....(3)}$$

and provides a direct measure of the local vorticity. Freestone used a vorticimeter of this type to measure the vorticity in a swirling jet and compared it with values obtained from direct measurement of the velocity field. Under these conditions he found that good correlation was obtained. Since the vortex to be investigated in the present tests is similar in nature, such a probe configuration will also be applicable in this type of flow.

Equation 3 assumes that the same calibration coefficient is applicable to each of the yawmeter pairs and Freestone obtained the average pressure differential by connecting left and right going tubes to a pair of manifolds and assuming that leakage effects would be small. During the construction of the yawmeters used in the present tests it was found difficult to achieve exactly equal calibration coefficients. This was accounted for by measuring the pressure differential across each pair of tubes individually, rather than averaging, and modifying equation 3 to:

$$\sum_{(i=1,j=8)(i=3,j=2)\ etc} \frac{1}{K_{i,j}}\Delta p_{i,j} = \rho\delta U(\frac{\partial w}{\partial y} - \frac{\partial v}{\partial z}) \quad \text{.....(4)}$$

4.2.1 Measurement of local flow properties other than vorticity

In addition to the local vorticity it was desired to obtain measurements of the local flow angularity, speed and total pressure. Since output was available from each pair of yawmeters it was possible to extract this information as follows.

A traverse was made with a pitot static tube in addition to the yawmeter. In this case pitot and static pressures were recorded separately. The pitot static tube was calibrated against flow angle and each pair of yawmeters calibrated against yaw for different angles of incidence, a typical calibration curve is shown in Fig 9. All required parameters could then be extracted using the iterative routine outlined in Fig 10. This routine was programmed to provide automatic data extraction on the controlling IBM. The system was proved by setting the probe cluster at predetermined angles to a known stream and checking that the recovered angle was equal to the setting angle.

5. Discussion of results

To date a full survey has been completed for the zero incidence case. The tests were made at a free stream velocity of 8 m/s corresponding to a Reynolds number of 1.35×10^5 based on the wing chord. The results of the flow visualisation tests are shown in Fig 2. As mentioned above, the oil flow tests show clearly that the flow on plate surface adjacent in the junction region and in the wake region downstream of the trailing edge is fed from the wing surface. The spreading of the wake region can be seen quite clearly in Fig 4.

Fig 5 shows the surface tufts and these illustrate the outward scouring on the plate surface caused by the formation of the vortex. This is in agreement with the expected flow structure reported, for example, in Ref 1.

Fig 11 shows contours of the local total vorticity, and Fig 12 the contours of local total pressure, at stations x/c = 1.199, 0.548, 0.467 and 0.142 downstream of the wing trailing edge. In each case the position of the wing centre line and maximum thickness is marked on the figure.

The total pressure contours (Fig 12) show clearly the boundary layer on the flat plate. It should be noted that the origin on the z coordinate is taken on the plate surface, but the closest traverse station was 10mm from the plate surface.

The vorticity contours show a region of strong vorticity for the station furthest from the wing trailing edge (Fig 11a). This reflects the spreading wake region illustrated in Fig 4. It can also be seen that the horseshoe vortex system appears to consist of a primary and a secondary system. This is consistent with the structure reported in Ref 5. The secondary vortex is caused by skewing of the wing boundary layer profile as a result of the cross flow. The primary vortex is situated near the plate surface while the secondary vortex is situated some distance above. This is shown best in the traverse nearest the trailing edge (Fig 11 d).

The structure is less clear in the total pressure contours (Fig 12). Here the picture is dominated by the loss in total pressure due to the wing wake.

6. Conclusions and Future Work

(a) Vorticity traverses downstream of the wing trailing edge confirm the existence of a primary and secondary horseshoe vortex system.

(b) The trailing vortex pair formed by the primary vortex move apart downstream of the wing trailing edge. This is consistent with observed oil film pictures.

(c) To date traverses have only been made with the wing at zero incidence. Further cases will be investigated with a lifting wing.

(d) The effect of filet geometry on the vortex formation will be investigated.

7. References

1. Ozcan O & Olcmen S, Measurements in the Wake of a Wing-Body Junction Bull. Tech Univ Istanbul Vol 40 pp 537-549, 1987

2. Bradshaw P & Shabaka I, Turbulent Flow Measurements in an Idealised Wing/Body Junction AIAA Paper 81-4028 AIAA Journal vol 19 No 2, 1981.

3. Kubendran I, McMahon H & Hubbartt J, Turbulent flow around a wing/fuselage type juncture. AIAA Journal vol 24 No 9, September 1986.

4. Glynn D R & Rawnsley S, Numerical Prediction of a Horseshoe Vortex Advances in Underwater Technology, Ocean Science and Offshore Engineering vol 15: Technology Common to Aero and Marine Engineering. Graham & Trotman 1988.

5. Kubendran I, McMahon H & Hubbartt J, Interference Drag in a Simulated Wing-Fuselage Juncture. Georgia Inst of Tech NASA Contractor Report 3811, 1984.

6. Kubendran I, McMahon H & Hubbartt J, Mean Velocities and Reynolds Stresses upstream of a simulated wing-fuselage juncture. Georgia Inst of Tech NASA Contractor Report 3695, 1983.

7. M M Freestone, Approximate measurement of streamwise vorticity in aeronautical flows by simple pressure probe. Conference publication Hatfield Polytechnic, Sept 1985.

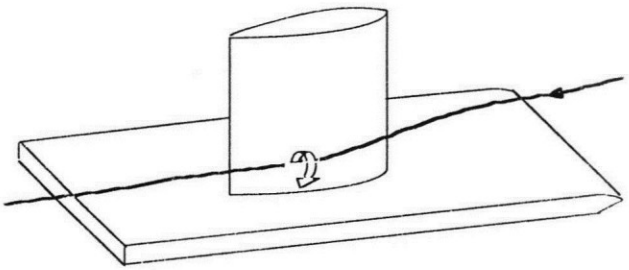

Fig 1. Formation of vortex

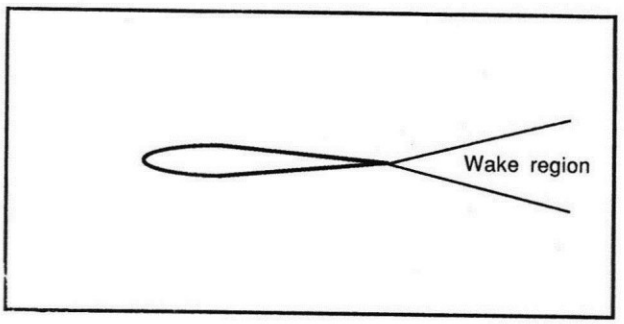

Fig 2. Spreading wake region

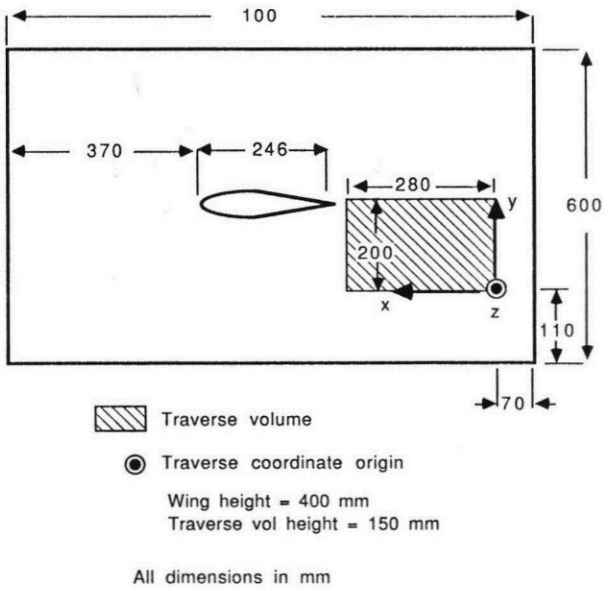

Fig 3. Traverse position

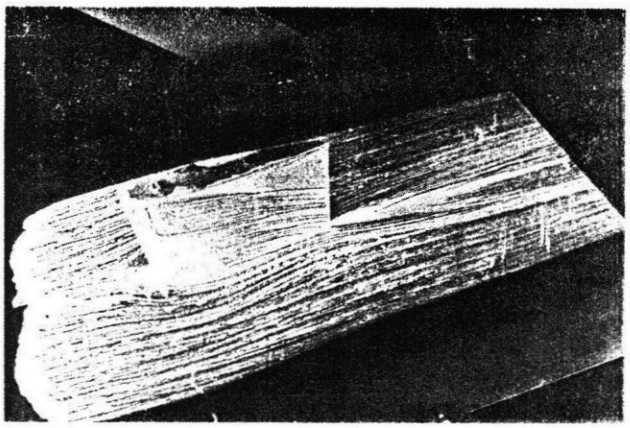

Fig 4. Oil flow

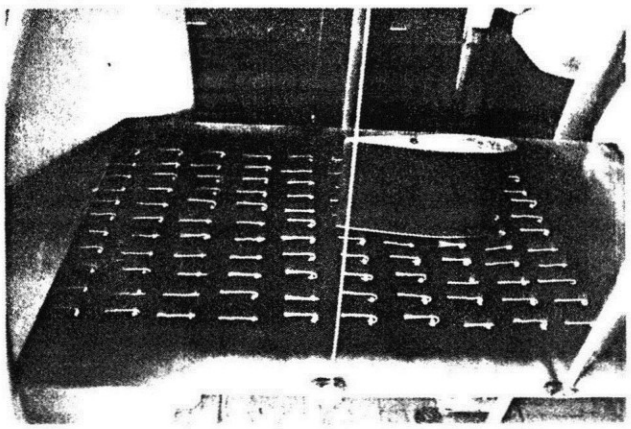

Fig 5. Surface tufts

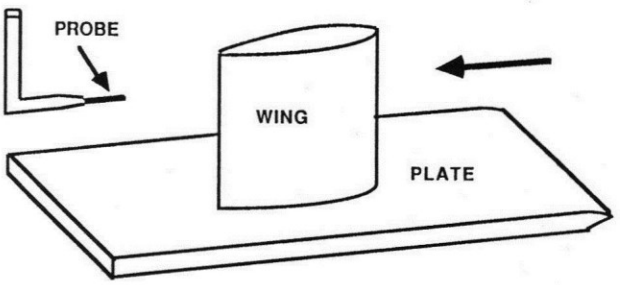

Fig 6. Probe location

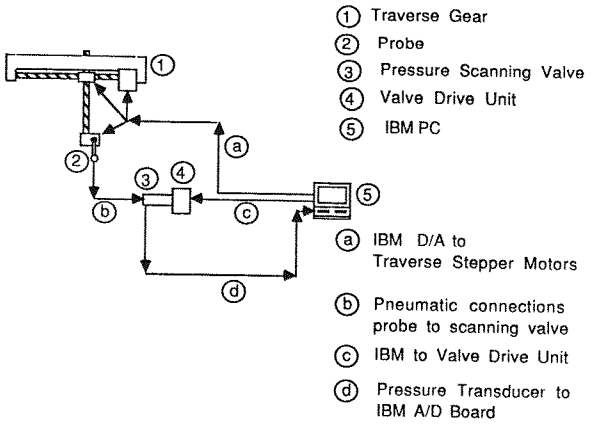

Fig 7. Control System

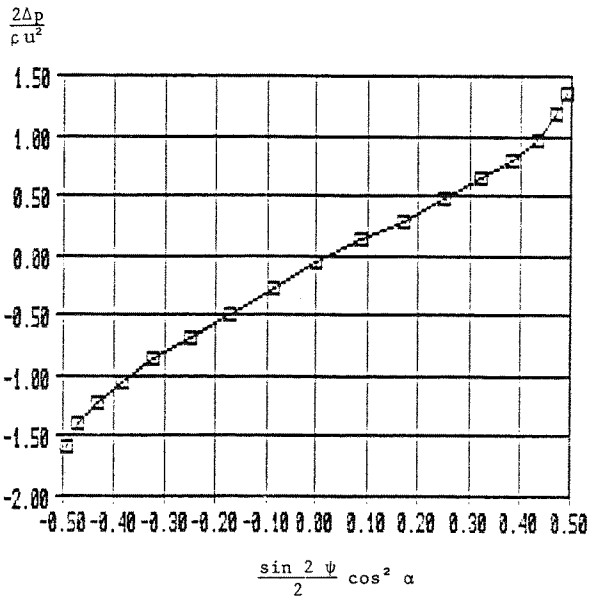

Fig 9. Typical yawmeter calibration curve

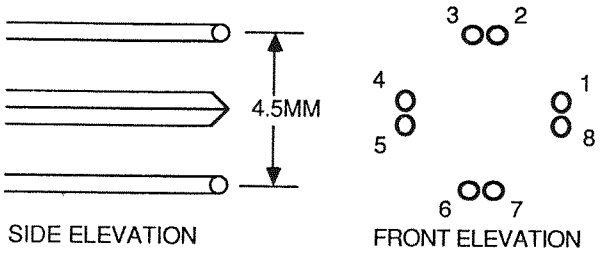

Fig 8. Yawmeter tube identification

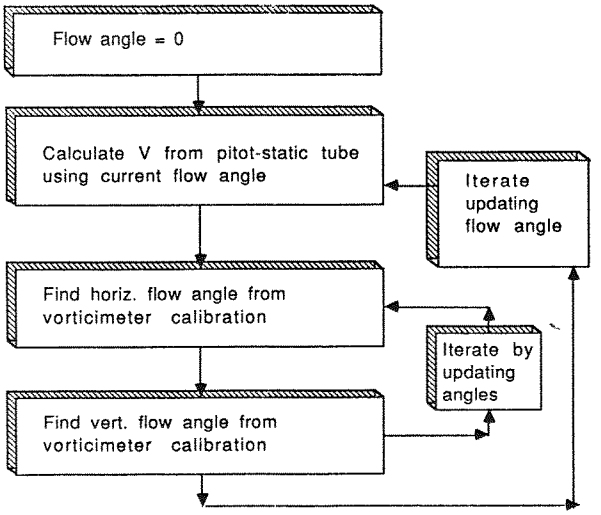

Fig 10. Flow chart showing data processing

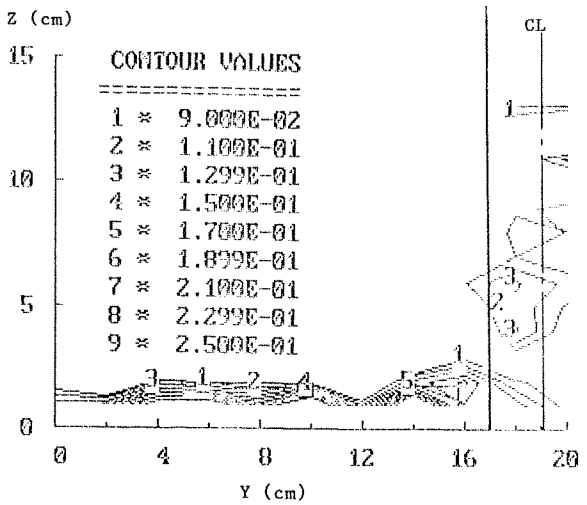

Fig 11a. Vorticity contours at x/c = 1.199

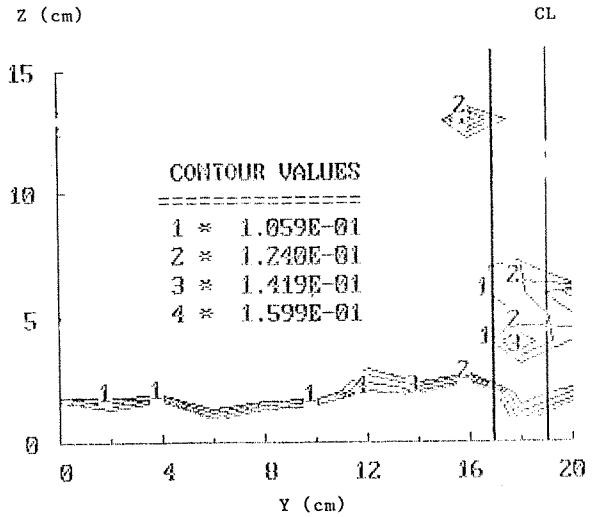

Fig 11b. Vorticity contours at x/c = 0.548

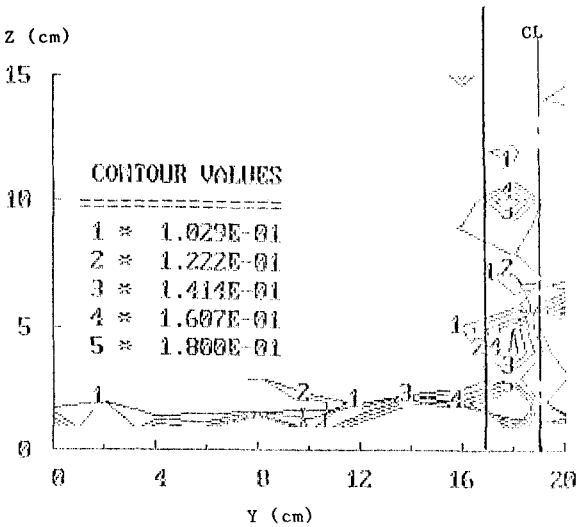

Fig 11c. Vorticity contours at x/c = 0.467

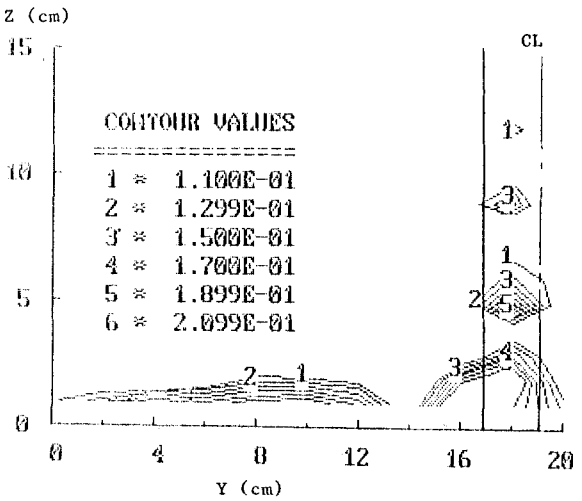

Fig 11d. Vorticity contours at x/c = 0.142

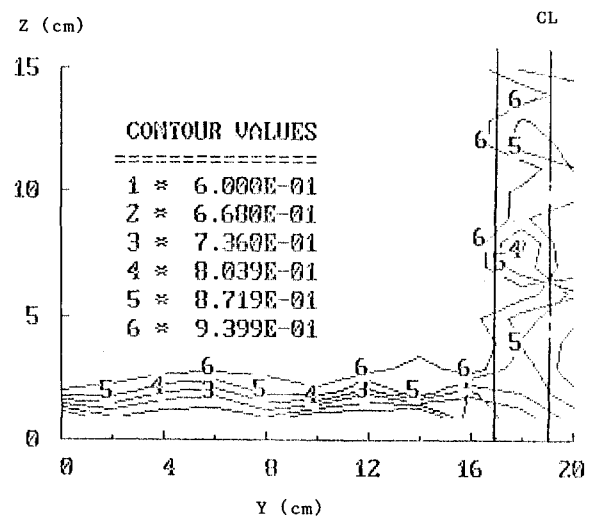

Fig 12a. Total pressure contours at x/c = 1.199

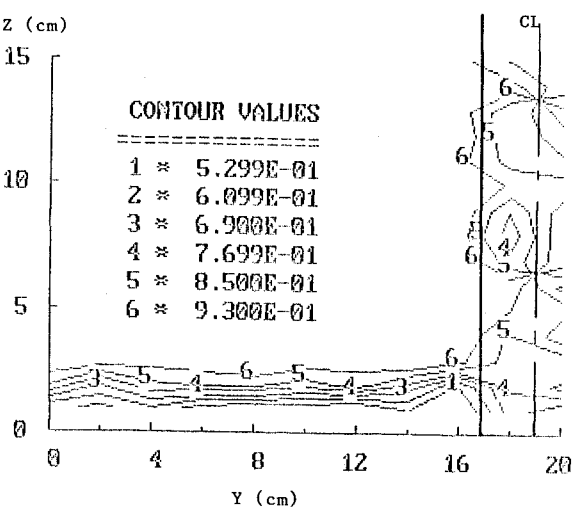

Fig 12b. Total pressure contours at x/c = 0.548

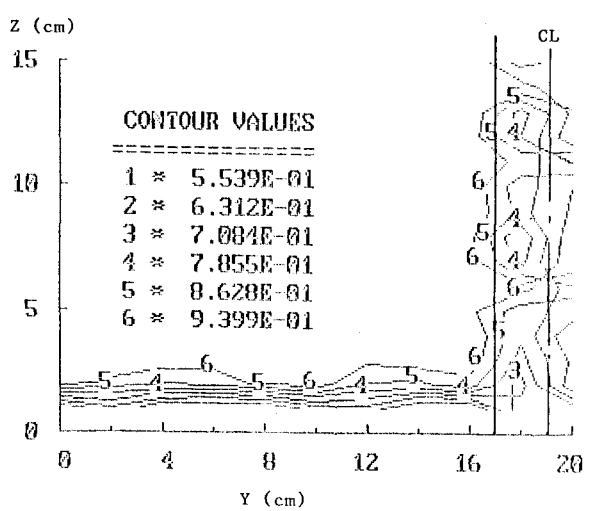

Fig 12c. Total pressure contours at x/c = 0.467

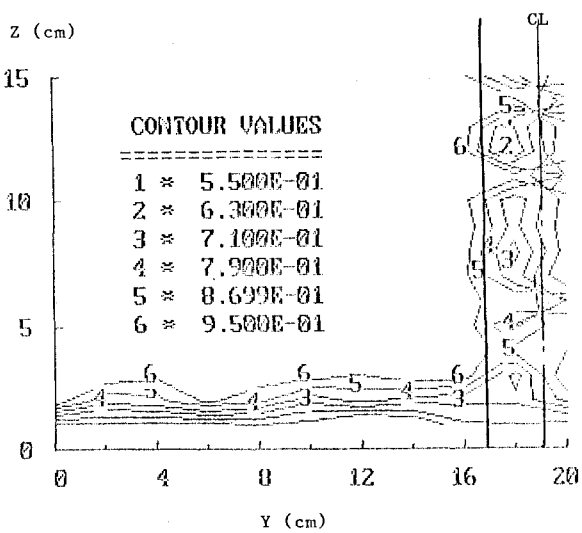

Fig 12d. Total pressure contours at x/c = 0.142